Removal of PCP-Na from aqueous systems using monodispersed pompon-like magnetic nanoparticles as adsorbents

Yu Liu, Hongbing Yu, Sihui Zhan, Shengjun Li, Hui Yang and Bo Liu

ABSTRACT

Novel monodispersed pompon-like magnetite/chitosan (Fe_3O_4/CS) composite nanoparticles were synthesized by a solvothermal method and used as adsorbents for the removal of toxic sodium pentachlorophenate (PCP-Na) from aqueous media. The adsorption behavior of PCP-Na on Fe_3O_4/CS obeyed the Langmuir isotherm and fitted the pseudo-second-order kinetics model. Thermodynamic parameters showed that the adsorption process was exothermic and spontaneous. Moreover, the adsorption was strongly pH-dependent. The results of XPS, thermodynamics, pH-dependent and desorption studies suggested that electrostatic attraction, hydrogen bonding and π-π interactions were all believed to play a role in PCP-Na adsorption on Fe_3O_4/CS. Having a saturation magnetization of 22.2 emu $\cdot$ g^{-1}, the Fe_3O_4/CS can be easily separated from water with magnets within 2 min. The adsorption equilibrium was achieved quite rapidly (within 30 min) and the maximum removal of PCP-Na (91.5%) was obtained at 25 °C and pH 6.5. The Fe_3O_4/CS investigated can be used to remove PCP-Na and other contaminants from wastewater.

Key words | adsorption, kinetics, mechanisms, PCP-Na, pompon-like magnetic nanoparticles, thermodynamics

Yu Liu (corresponding author)
State Key Laboratory of Simulation and Regulation of Water Cycle in River Basin,
China Institute of Water Resources and Hydropower Research,
Fuxing Road A1,
Haidian District, Beijing 100038,
China
E-mail: *liuyu@tjhri.com*

Yu Liu
Hongbing Yu
Sihui Zhan
College of Environmental Science and Engineering,
Nankai University,
Weijin Road 94,
Nankai District, Tianjin 300071,
China

Yu Liu
Shengjun Li
Hui Yang
Bo Liu
Tianjin Hydraulic Science Research Institute,
Youyi Road 60,
Hexi District, Tianjin 300061,
China

INTRODUCTION

Pentachlorophenol (PCP) and its salts, most notably sodium pentachlorophenate (PCP-Na), are widely used as biocides for the protection of timber and textiles all over the world (Muir & Eduljee 1999). PCP and its salts have attracted great attention worldwide and have been listed as priority pollutants by the US Environmental Protection Agency owning to their toxicity, endocrine-disturbing effect, mutagenicity, carcinogenicity, and bioaccumulation (Keith & Telliard 1979). Therefore it is of great importance to develop efficient technologies to remove PCP and its salts.

Adsorption to solid phases is a key process for the environmental fate of potentially toxic and bioaccumulative pollutants. Numerous adsorbents such as carbon black (Domínguez-Vargas *et al*. 2009), pumice (Akbal 2005), zeolite (Kuleyin 2007), and activated carbon (Diaz-Flores *et al*. 2006) were developed for removing chlorophenols. However, the dispersion limitation and recovery difficulty of these adsorbents limit their practical applications. Therefore, in order to obtain effective adsorption result and not to cause secondary environmental contamination, the extended dispersity and the facile separation of nano-adsorbents are very important.

Although the biomedical applications of magnetic nanoparticles have been extensively investigated (Bulte *et al*. 2001; Nam *et al*. 2003), few applications in the environmental field have been reported. The facile separation of magnetic nano-adsorbents provide efficient and cost-effective approaches for the removal of contaminants. Bare magnetite nanoparticles are susceptible to air oxidation and are easily aggregated in aqueous systems (Maity & Agrawal 2007). Chitosan is a natural polysaccharide with many useful features such as hydrophilicity, biocompatibility, biodegradability, antibacterial properties and a remarkable affinity for many biomacromolecules. Thus, chitosan-modified Fe_3O_4 nanoparticles will probably yield a novel magnetic adsorbent for the efficient removal of contaminants.

The aim of this work was the production of an new adsorptive material (magnetite/chitosan, Fe_3O_4/CS), and the feasibility of using this new adsorbent for PCP-Na

doi: 10.2166/wst.2013.557

removal from water. The adsorption behavior of PCP-Na onto Fe_3O_4/CS nanoparticles was evaluated with respect to the adsorption isotherm, thermodynamics, kinetics and effects of pH. In addition, the possible adsorption mechanisms of PCP-Na onto Fe_3O_4/CS is also described.

MATERIALS AND METHODS

Preparation and characterization of magnetic nano-adsorbents

Fe_3O_4/CS nanoparticles were prepared by a solvothermal method (Zhou *et al.* 2009). As a comparison, Fe_3O_4 nanoparticles without modification of chitosan were prepared in a similar way without the addition of chitosan. All reagents used in the experiments, detailed synthesis procedure and characterization of the prepared nanoparticles were described in the Supplementary data (available online at http://www.iwaponline.com/wst/068/557.pdf).

Adsorption studies

A PCP-Na (1.0 g L^{-1}) solution was prepared by mixing PCP with NaOH (0.3 g L^{-1}) and stored in a dark-brown glass bottle to avoid any photochemical reactions. In a typical adsorption experiment, a measured amount of the as-prepared Fe_3O_4/CS nanoparticles were added into 100 mL of PCP-Na solution (50–200 mg L^{-1}). The pH of the PCP-Na solution was adjusted to the desired values with HCl and NaOH. The suspensions were stirred continuously in a thermostatic shaker at 250 rpm and at constant temperatures of 25, 35 or 45 °C respectively. At equilibrium time or given time intervals, the Fe_3O_4/CS nanoparticles with absorbed PCP-Na were separated from the mixture with a magnet. The concentration of PCP-Na in the aqueous solution was analyzed with a UV-Visible spectrophotometer (Varian, Cary 50 Conc, USA), and the absorbance of PCP-Na solution was measured at a wavelength of 320 nm.

RESULTS AND DISCUSSION

Characterization of magnetic nano-adsorbents

Figure S1a in the Supplementary data (available online at http://www.iwaponline.com/wst/068/557.pdf) shows the X-ray diffraction (XRD) patterns for the Fe_3O_4 and Fe_3O_4/CS nanoparticles. Similar XRD patterns indexed to Fe_3O_4 (JCPDS: 65–3107) were observed for both samples. It revealed that the modification with chitosan did not result in the phase change of Fe_3O_4. Comparing with the Fe_3O_4, the diffraction peaks of Fe_3O_4/CS were shorter and blunter, indicating that particle sizes were smaller. The results showed that the chitosan modification could clearly hinder the increase of the Fe_3O_4 crystallite size. Figure S1b (available online at http://www.iwaponline.com/wst/068/557.pdf) presents the Fourier transform infrared (FTIR) spectra of pure chitosan and Fe_3O_4/CS. The pure chitosan can be characterized by the broad peak over the region of 3,200–3,500 cm^{-1} (O–H stretching and N–H stretching vibrations), 1,660 and 1,592 cm^{-1} (amide I and amide II bands), and 1,150 cm^{-1} (C–O–C stretching vibrations), which is consistent with previous reports (Lawrie *et al.* 2007). All these characteristic bands can also be seen in the spectrum of Fe_3O_4/CS. The band that appears at 608 cm^{-1} can be related to Fe–O vibration (Ge *et al.* 2007). These results indicate the presence of chitosan on the as-synthesized Fe_3O_4/CS nanoparticles.

Figure 1 shows the transmission electron microscopy (TEM) images of the as-prepared Fe_3O_4 and Fe_3O_4/CS nanoparticles. It is observed that the diameter of the spherical Fe_3O_4 is 200–350 nm and the microspheres aggregate; see Figure 1(a). The BET specific surface area was 6.35 m^2/g. As for the Fe_3O_4/CS nanoparticles, it was noteworthy that a novel pompon-like structure was produced. The Fe_3O_4/CS nanoparticles were well monodispersed with diameters of 100–200 nm, see Figure 1(b), and the specific surface area for the Fe_3O_4/CS was 32.18 m^2/g. The increased BET surface area of the Fe_3O_4/CS compared to the Fe_3O_4 might be ascribed to their greater dispersity, smaller particle size and increased surface roughness. As shown in Figure 1, the Fe_3O_4/CS was pompon-like in structure and the surface roughness of the Fe_3O_4/CS was significantly higher compared to the Fe_3O_4. Therefore, the maximum adsorption result of PCP-Na by using Fe_3O_4/CS nanoparticles as an adsorbent is reasonable, and has been validated in the following experiments.

The superparamagnetic properties of the Fe_3O_4 and Fe_3O_4/CS were verified with the magnetization curve measured by a vibrating sample magnetometer (VSM). The magnetization curve (Figure S2 in the Supplementary data, available online at http://www.iwaponline.com/wst/068/557.pdf) exhibited zero remanence and coercivity, and follows the Langevin function, which indicated that the prepared Fe_3O_4 and Fe_3O_4/CS were superparamagnetic. The respective saturation magnetizations of Fe_3O_4/CS and Fe_3O_4 were 22.2 and 22.3 emu g^{-1}, suggesting that no change of the saturation magnetization was observed after

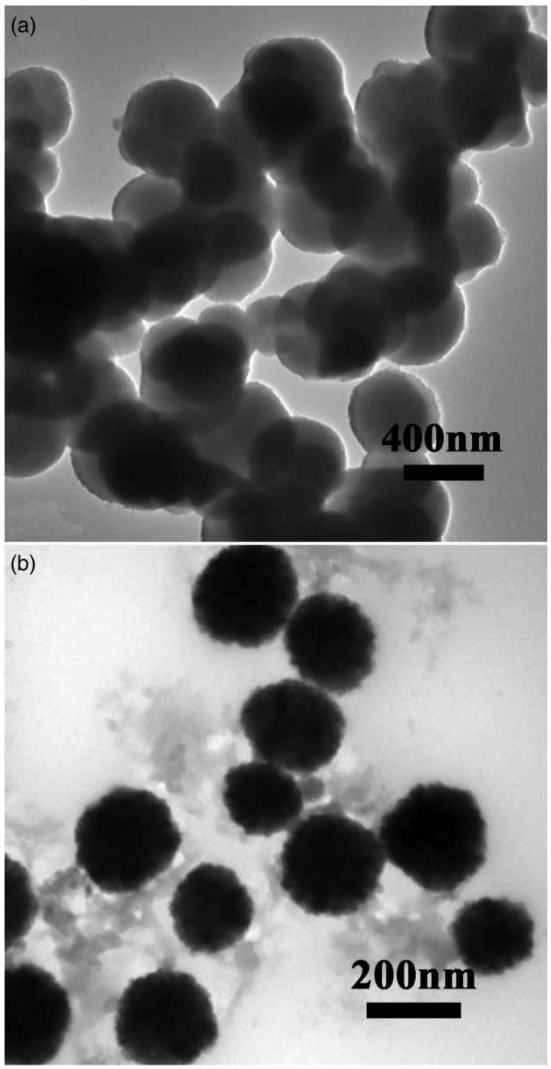

Figure 1 | TEM images of the prepared Fe_3O_4 (a) and Fe_3O_4/CS (b).

modification with chitosan. Separation of Fe_3O_4/CS from its aqueous dispersions can be easily carried out within 2 min with a magnet. Therefore, the facile separation of Fe_3O_4/CS makes its future application viable.

Adsorption equilibrium and effect of adsorbent dose

The adsorption experiment was studied at pH 6.5, 25 °C, and an initial PCP-Na concentration of 100 mg L^{-1} (Figure S3 of the Supplementary data, available online at http://www.iwaponline.com/wst/068/557.pdf). It is worth noting that the adsorption equilibrium was reached quite rapidly (within 30 min). By contrast, the adsorption of PCP from aqueous solutions by activated sludge biomass (Wang *et al.* 2000), dolomitic sorbents (Marouf *et al.* 2006) and (M) Al-MCM-41 ($M = Na^+$, K^+, Cu^{2+}, Cr^{3+}) (Marouf-Khelifa *et al.* 2004) showed that their equilibriums were attained after 2 h. According to the literature (Akbal 2005; Diaz-Flores *et al.* 2006; Domínguez-Vargas *et al.* 2009; Kuleyin 2007), chlorophenol adsorption reached equilibrium after more than 24 h. According to these results, it is clear that the novel pompon-like Fe_3O_4/CS nanoparticles have great potential to act as effective adsorbents.

As shown in Figure S3, the adsorbent (Fe_3O_4/CS) dose significantly influenced the adsorption of PCP-Na. The PCP-Na removal was 70.0% for 0.15 g of Fe_3O_4/CS, and it increased greatly to 91.5% for 0.28 g of Fe_3O_4/CS. However, a further increase in adsorbent amount showed no positive effect on removal. Hence an optimum adsorbent dose (2.8 g L^{-1}) was chosen in this work. A comparison of PCP-Na removal using Fe_3O_4/CS and Fe_3O_4 as adsorbents in the same conditions is illustrated in the inset of Figure S3. The maximum removal observed by using the Fe_3O_4 adsorbent was 69.2%, and the time required to achieve adsorption equilibrium was almost 2 h. The rapid and obvious adsorption result demonstrated the feasibility and superiority of Fe_3O_4/CS as an effective adsorbent for removing PCP-Na from water.

Adsorption isotherms

The equilibrium isotherms for the adsorption of PCP-Na on Fe_3O_4/CS at various temperatures (25, 35 and 45 °C) were obtained at pH 6.5 by varying the initial concentration of PCP-Na from 50 to 200 mg L^{-1} (Figure 2). The adsorption data were analyzed according to the Langmuir isotherm as follows (Wang *et al.* 2013):

$$\frac{C_e}{q_e} = \frac{1}{Kq_m} + \frac{C_e}{q_m} \quad (1)$$

where q_e is the adsorption capacity (mg g^{-1}) based on the dry weight of adsorbent, C_e is the equilibrium concentration (mg L^{-1}) in solution, q_m is the maximum adsorption capacity (mg g^{-1}), and K is the Langmuir adsorption equilibrium constant (L mg^{-1}). As illustrated in Figure 2(b), plotting of C_e/q_e against C_e at various temperatures yielded straight lines, revealing that the adsorption of PCP-Na on Fe_3O_4/CS obeyed the Langmuir adsorption. As shown in Table S1 in the Supplementary data (available online at http://www.iwaponline.com/wst/068/557.pdf), the value of K decreased with the increase of temperatures, which confirmed the adsorption process was exothermic in nature (Hu *et al.* 2005).

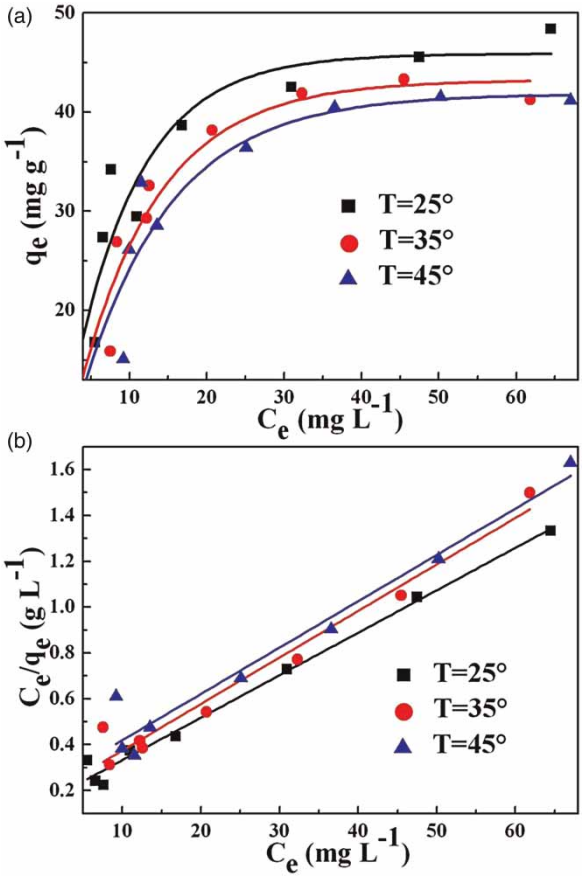

Figure 2 | Adsorption of PCP-Na on Fe_3O_4/CS at 25, 35 and 45 °C (pH 6.5). (a) Adsorption isotherm; (b) Langmuir linear fitting.

Adsorption thermodynamics

The adsorption thermodynamics was investigated at pH 6.5, 25–50 °C, with an initial PCP-Na concentration of 100 mg L^{-1}, see Figure 3(a). As shown in Figure 3(a), the adsorption capacity of PCP-Na decreased with increasing temperature. Plotting ln (q_e/C_e) against $1/T$ is shown in the inset of Figure 3(a) and the thermodynamic parameters are listed in Table 1. The negative enthalpy change ($\Delta H = -20.81$ kJ mol^{-1}) further confirmed an exothermic adsorption process as observed in the above adsorption isotherms. Furthermore, the negative values of entropy change (ΔS) and Gibbs energy change (ΔG) indicated a spontaneous adsorption process driven by enthalpy change (Li *et al.* 2011).

Adsorption kinetics

In order to further investigate the adsorption process, the pseudo-first-order kinetics model and pseudo-second-order kinetics model were used to test the adsorption kinetics data. The pseudo-first-order and pseudo-second-order equations are given as Equations (2) and (3) respectively (Ioannou *et al.* 2013):

$$\log(q_e - q_t) = \log q_e - \frac{k_1}{2.303}t \quad (2)$$

$$\frac{t}{q_t} = \frac{1}{k_2 q_e^2} + \frac{1}{q_e}t \quad (3)$$

where q_e and q_t are the amount of PCP-Na adsorbed on the adsorbent (mg g^{-1}) at equilibrium and at time t (min), respectively, k_1 and k_2 are the adsorption rate constants of pseudo-first-order (min^{-1}) and pseudo-second-order (mg $g^{-1} \cdot min^{-1}$) respectively.

Figure 3(b) shows the adsorption kinetics of PCP-Na on Fe_3O_4/CS at 25, 35 and 45 °C. And the pseudo-first- and pseudo-second-order constants and correlation coefficients (R^2) are shown in Table 2. According to the results in Table 2, the pseudo-second-order adsorption model was more suitable for describing the adsorption kinetics of PCP-Na on Fe_3O_4/CS.

Effect of initial pH

The effect of initial pH on the adsorption of PCP-Na by Fe_3O_4/CS was investigated at 25 °C and an initial PCP-Na concentration of 100 mg L^{-1}. Given the solubility limit at lower pH values, the pH of the PCP-Na solution were adjusted to the desired values of 6.5, 7, 8, 9, and 10. As seen in Figure 3(c), PCP-Na adsorption on the Fe_3O_4/CS was reduced by the increasing pH. According to the zeta-potential analysis (Figure S4 in the Supplementary data, available online at http://www.iwaponline.com/wst/068/557.pdf), the Fe_3O_4/CS is negatively charged in the pH range of 6.5–10, and more PCP^- anions are repelled from the Fe_3O_4/CS surface by repulsive electrostatic interactions when the pH is increased. As a result, PCP-Na removal decreases with the increase in pH. However, the optimum removal at pH 6.5 could not be well explained by the Zeta-potential study. Therefore, several important implications can be drawn from the results of pH effects: (i) the PCP-Na adsorption to Fe_3O_4/CS is strongly pH-dependent; (ii) the PCP-Na adsorption process could not be explained solely on the basis of electrostatic interactions (attraction or repulsion); and thus (iii) there must be more than one mechanism responsible for PCP-Na removal on Fe_3O_4/CS.

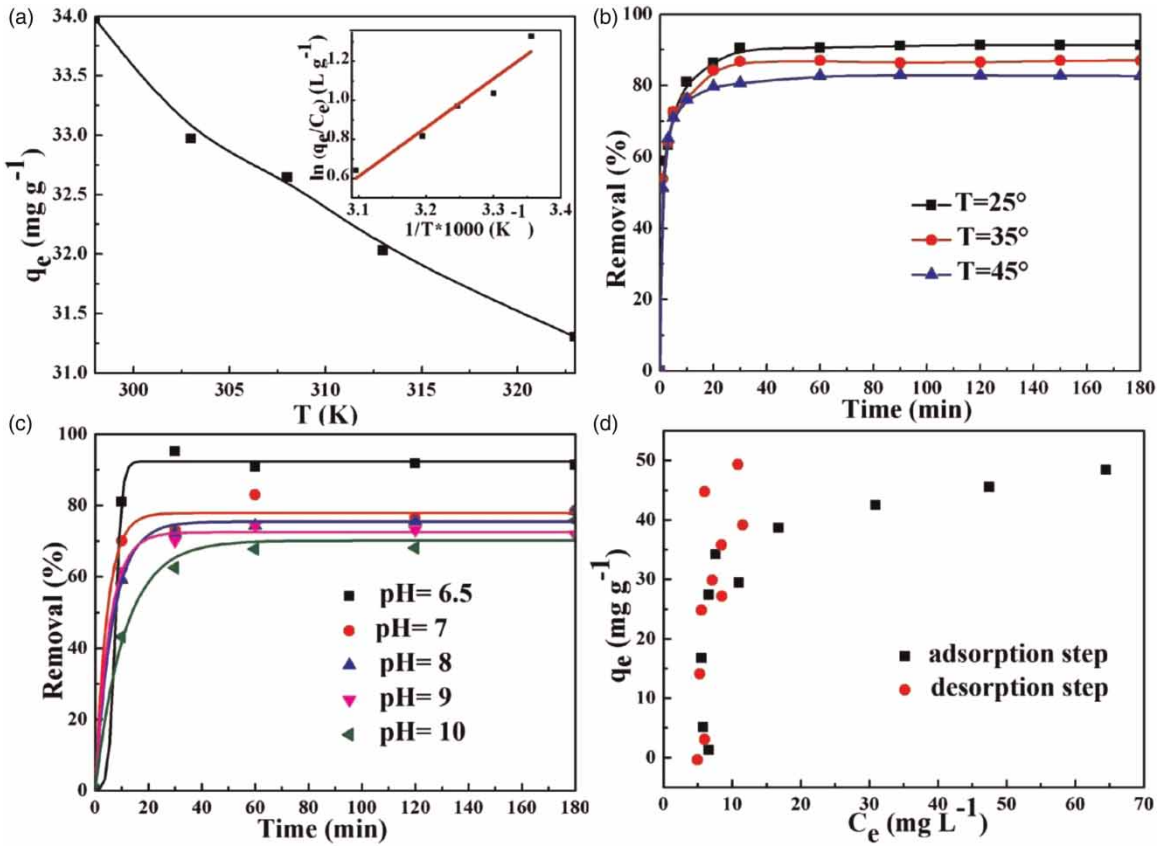

Figure 3 | (a) Adsorption thermodynamics of PCP-Na on Fe_3O_4/CS (pH 6.5). (b) Adsorption kinetics of PCP-Na on Fe_3O_4/CS at 25, 35 and 45 °C (pH 6.5). (c) Effect of pH on the adsorption of PCP-Na by Fe_3O_4/CS at 25 °C. (d) Adsorption and desorption isotherm of PCP-Na on Fe_3O_4/CS at pH 6.5 and 25 °C.

Table 1 | Thermodynamic parameters of adsorption at pH 6.5 and different temperatures

Temperatures (°C)	ln$K$ ln (q_e/C_e)	ΔG (kJ mol^{-1}) $-RT$ ln K	ΔH (kJ mol^{-1})	ΔS (J mol$^{-1}\cdot$K^{-1}) ($\Delta H-\Delta G$) /T
25	1.33	− 3.30	− 20.81	− 58.76
30	1.03	− 2.61		− 60.07
35	0.97	− 2.49		− 59.48
45	0.75	− 1.97		− 59.25
50	0.64	− 1.72		− 59.10

Adsorption mechanisms

X-ray photoelectron spectroscopy (XPS) analysis for Fe_3O_4/CS before and after adsorption of PCP-Na at pH 6.5, 25 °C, and an initial PCP-Na concentration of 100 mg L^{-1} were used to further elaborate the adsorption of PCP^- on the Fe_3O_4/CS. The presence of the Cl (2p) peak on the Fe_3O_4/CS after the adsorption experiment suggested that PCP^- adheres to the surface of Fe_3O_4/CS

Table 2 | Comparison of first- and second-order kinetic adsorption models

		First-order kinetic model			Second-order kinetic model		
Temperatures (°C)	$q_{e.exp}$ (mg g^{-1})	$k_1\times10^3$ (min^{-1})	$q_{e.cal}$ (mg g^{-1})	R^2	$k_2\times10^3$ (mg g^{-1} min^{-1})	$q_{e.cal}$ (mg g^{-1})	R^2
25	33.98	45.60	9.12	0.9533	23.86	34.25	>0.9999
35	32.65	23.49	9.78	0.8594	33.99	32.52	>0.9999
45	30.61	63.45	7.85	0.9129	37.60	30.84	>0.9999

(Figure S5 in the Supplementary data, available online at http://www.iwaponline.com/wst/068/557.pdf). The XPS distribution of the iron and oxide in the samples after adsorption are in good agreement with the values of the samples before adsorption. It can be deduced that no chemical redox reaction occurred during the whole process. For the Fe_3O_4/CS studied here, it may be expected that the excellent adsorption characteristics were most likely due to the large number of hydroxyl groups and primary amino groups in chitosan. These groups could act as adsorption sites with high activity. However, given the above results of the effects of pH, it was deduced that the mechanisms responsible for this adsorption process might be complicated. Therefore, the mechanisms of this adsorption system were elaborated as follow.

First, the removal of PCP-Na decreased as the pH increased from 6.5 to 10, which could be attributed to the electrostatic repulsion existing between the Fe_3O_4/CS surface and the PCP^- in solution. PCP-Na was present as PCP^- ($C_6H_5Cl_5$–O^-) when the pH was above 6. On the other hand, changes in pH can induce the protonation or deprotonation of R–NH_2 of chitosan relative to its pKa values of 6.3–6.7 (Equations (4) and (5)) (Yan & Bai 2005).

$$\text{R-NH}_2 + \text{H}^+ \leftrightarrow \text{R-NH}_3^+ \tag{4}$$

$$\text{R-NH}_3^+ + \text{C}_6\text{H}_5\text{Cl}_5\text{–O} \leftrightarrow \text{R-NH}_3^+\text{O}^-\text{–C}_6\text{H}_5\text{Cl}_5 \tag{5}$$

At lower pH conditions (pH = 6.5), more amino groups were protonated, and thus reaction of Equation (4) proceeded to the right. At higher pH values, OH^- ions may be adsorbed to the surface of Fe_3O_4/CS through a hydrogen bond, which contributes to the following reaction:

$$\text{R-NH}_2 + \text{OH}^- \rightarrow \text{R-NH}_2 \cdots \text{OH}^- \tag{6}$$

The action of Equation (6) reduces the combination of the amino group with the negatively charged PCP^- by weak chemical action, see Equation (5). Given that the intensity of the electrostatic repulsion varies with pH values, it was assumed that the contribution of the electrostatic mechanism varies with pH.

In addition, the hydroxyl group present in the PCP^- ring might combine through hydrogen bonds with the hydroxyl group on the chitosan surface, which was controlled by the limited number of available vacant sites on the chitosan surface (Lawrie *et al.* 2007). The magnitude of ΔH, related to the sorption energy, can indicate the type of binding mechanism involved, i.e., physical and/or chemical adsorption.

Energies of 4–8 kJ mol^{-1} are required by Van der Waals interactions compared to energies of 8–40 kJ mol^{-1}, which correspond to hydrogen bonding (DiVincenzo & Sparks 2001). The calculated ΔH value (20.81 kJ mol^{-1}) of the present study was 8–40 kJ mol^{-1}, which was indicative of the hydrogen bonding interactions between the PCP-Na and the Fe_3O_4/CS surface. On this consideration, the adsorption of PCP-Na was partly due to hydrogen bonding.

Furthermore, it was reported that π-π interactions control the adsorption of phenol and chlorophenols on granular activated carbons (Jung *et al.* 2001; El-Sheikh *et al.* 2004). The chloro group is an electron-withdrawing group and therefore, the electron density in an aromatic ring decreases as the number of chloro group increases. As a result, PCP-showed the highest affinity to the π-electrons in chitosan. It meant that PCP-Na may be adsorbed on to the Fe_3O_4/CS surface through π-π interactions due to the dispersion forces between the π electrons in the aromatic ring of the PCP^- and the π electrons in the aromatic rings of the chitosan in Fe_3O_4/CS. To confirm the mechanism of π-π interactions, desorption of the PCP-Na adsorbed on Fe_3O_4/CS at pH 6.5 and 25 °C was conducted. The adsorbates adsorbed on to the Fe_3O_4/CS were desorbed by placing the Fe_3O_4/CS loaded with adsorbates in an aqueous solution without PCP-Na. Under these conditions, the adsorbates were transferred from the Fe_3O_4/CS to the solution until a new equilibrium reached. The results of the adsorption–desorption process are shown in Figure 3(d). It can be noted that the experimental data of adsorption and desorption processes were mostly on the same isotherm, except the data obtained from the higher initial PCP-Na concentration. Because of their weak attraction forces, it was reported that the adsorption caused by π-π interactions is reversible (Diaz-Flores *et al.* 2006). In other words, if the adsorption process was caused by the dispersion forces between the π electrons, the new equilibrium reached in the desorption step would be the same as that of the adsorption step. The desorption experiment here demonstrated that the π-π interactions played a role in the adsorption but the intensity of π-π interactions was weak at the higher initial PCP-Na concentration.

Given the above results, therefore, the adsorption of PCP-Na by Fe_3O_4/CS appears to be a complex process,

and the adsorption mechanisms involve electrostatic attraction, hydrogen bonding and π-π interactions.

CONCLUSION

Novel monodispersed pompon-like magnetic Fe_3O_4/CS nanoparticles were successfully produced by a solvothermal method. The prepared Fe_3O_4/CS was used as adsorbents to remove PCP-Na from aqueous solutions. The adsorbents can be well dispersed in the aqueous solution and be easily separated from the solution with a magnet after adsorption. The adsorption equilibrium was achieved quite rapidly (within 30 min) and the maximum removal of PCP-Na (91.5%) was obtained at 25 °C and pH 6.5. The PCP-Na removal was strongly pH-dependent. The negative values of ΔG and ΔH showed that the adsorption was a spontaneous and exothermic process. The adsorption follows the Langmuir isotherm and the pseudo-second-order kinetics model. The adsorption mechanism can be summarized as the combined effects of electrostatic attraction, hydrogen bonding and π-π interactions. It is expected that the Fe_3O_4/CS has great potential for removal of contaminants from aqueous media.

ACKNOWLEDGEMENTS

The authors gratefully acknowledge the financial support of Open Research Fund of State Key Laboratory of Simulation and Regulation of Water Cycle in River Basin (China Institute of Water Resources and Hydropower Research) (IWHR-SKL-201201), Special Research of Public Industry (Ministry of Water Resources of China) (201101059), and National Natural Science Foundation of China (20907022 and 21003094).

REFERENCES

Akbal, F. 2005 Sorption of phenol and 4-chlorophenol onto pumice treated with cationic surfactant. *J. Environ. Manage.* **74**, 239–244.

Bulte, J. W. M., Douglas, T., Witwer, B., Zhang, S. C., Strable, E., Lewis, B. K., Zywicke, H., Miller, B., Van Gelderen, P., Moskowitz, B. M., Duncan, I. D. & Frank, J. A. 2001 Magnetodendrimers allow endosomal magnetic labeling and *in vivo* tracking of stem cells. *Nat. Biotechnol.* **19**, 1141–1147.

Diaz-Flores, P. E., Leyva-Ramos, R., Guerrero-Coronado, R. M. & Mendoza-Barron, J. 2006 Adsorption of pentachlorophenol from aqueous solution onto activated carbon fiber. *Ind. Eng. Chem. Res.* **45**, 330–336.

DiVincenzo, J. P. & Sparks, D. L. 2001 Sorption of the neutral and charged forms of pentachlorophenol on soil: evidence for different mechanisms. *Arch. Environ. Contam. Toxicol.* **40**, 445–450.

Domínguez-Vargas, J. R., Navarro-Rodríguez, J. A., Beltrán de Heredia, J. & Cuerda-Correa, E. M. 2009 Removal of chlorophenols in aqueous solution by carbon black low-cost adsorbents. Equilibrium study and influence of operation conditions. *J. Hazard. Mater.* **169**, 302–308.

El-Sheikh, A. H., Newman, A. P., Al-Daffaee, H. K., Phull, S. S. & Lynch, D. E. 2004 The use of activated carbons with basic properties for the treatment of 2-chlorophenols. *Adsorpt. Sci. Technol.* **22**, 451–465.

Ge, J. P., Hu, Y. X., Biasini, M., Beyermann, W. P. & Yin, Y. D. 2007 Superparamagnetic magnetite colloidal nanocrystal clusters. *Angew. Chem. Int. Ed.* **46**, 4342–4345.

Hu, J., Chen, G. & Lo, I. M. C. 2005 Removal and recovery of Cr (VI) from wastewater by maghemite nanoparticles. *Water Res.* **39**, 4528–4536.

Ioannou, Z., Karasavvidis, Ch., Dimirkou, A. & Antoniadis, V. 2013 Adsorption of methylene blue and methyl red dyes from aqueous solutions onto modified zeolites. *Water Sci. Technol.* **67** (5), 1129–1136.

Jung, M. W., Ahn, K. H., Lee, Y. H., Kim, K. P., Rhee, J. S., Park, J. T. & Paeng, K. J. 2001 Adsorption characteristics of phenol and chlorophenols on granular activated carbons (GAC). *Microchem. J.* **70**, 123–131.

Keith, L. H. & Telliard, W. A. 1979 ES&T special report: priority pollutants. I. A perspective view. *Environ. Sci. Technol.* **13**, 416–423.

Kuleyin, A. 2007 Removal of phenol and 4-chlorophenol by surfactant-modified natural zeolite. *J. Hazard. Mater.* **144**, 307–315.

Lawrie, G., Keen, I., Drew, B., Chandler-Temple, A., Rintoul, L., Fredericks, P. & Grøndahl, L. 2007 Interactions between alginate and chitosan biopolymers characterized using FTIR and XPS. *Biomacromolecules* **8**, 2533–2541.

Li, X., Liu, R., Wu, S., Liu, J., Cai, S. S. & Chen, D. S. 2011 Efficient removal of boron acid by N-methyl-D-glucamine functionalized silica-polyallylamine composites and its adsorption mechanism. *J. Colloid. Interface Sci.* **361**, 232–237.

Maity, D. & Agrawal, D. C. 2007 Synthesis of iron oxide nanoparticles under oxidizing environment and their stabilization in aqueous and non-aqueous media. *J. Magn. Magn. Mater.* **308**, 46–55.

Marouf, R., Khelifa, N., Marouf-Khelifa, K., Schott, J. & Khelifa, A. 2006 Removal of pentachlorophenol from aqueous solutions by dolomitic sorbents. *J. Colloid. Interface Sci.* **297**, 45–53.

Marouf-Khelifa, K., Khelifa, A., Belhakem, A., Marouf, R., Abdelmalek, F. & Addou, A. 2004 The adsorption of pentachlorophenol from aqueous solutions onto exchanged Al-MCM-41 materials. *Adsorpt. Sci. Technol.* **22**, 1–12.

Muir, J. & Eduljee, G. 1999 PCP in the fresh water and marine environment of the European union. *Sci. Total Environ.* **236**, 41–56.

Nam, J. M., Thaxton, C. S. & Mirkin, C. A. 2003 Nanoparticle-based bio-bar codes for the ultrasensitive detection of proteins. *Science* **301**, 1884–1886.

Wang, J. L., Qian, Y., Horan, N. & Stentiford, E. 2000 Bioadsorption of pentachlorophenol (PCP) from aqueous solution by activated sludge biomass. *Bioresour. Technol.* **75**, 157–161.

Wang, S. C., Yuan, R. Z., Yu, X. Y. & Mao, C. J. 2013 Adsorptive removal of phosphate from aqueous solutions using lead-zinc tailings. *Water Sci. Technol.* **67** (5), 983–988.

Yan, W. L. & Bai, R. 2005 Adsorption of lead and humic acid on chitosan hydrogel beads. *Water Res.* **39**, 688–698.

Zhou, Y. X., Yao, H. B., Gong, J. Y., Liu, S. J. & Yu, S. H. 2009 Hierarchical $FeWO_4$ microcrystals: solvothermal synthesis and their photocatalytic and magnetic properties. *Inorg. Chem.* **48**, 1082–1090.

First received 20 May 2013; accepted in revised form 13 September 2013. Available online 24 October 2013